

# Topological quantum phase transitions and topological flat bands on the star lattice

Wen-Chao Chen,<sup>1</sup> Ru Liu,<sup>1</sup> Yi-Fei Wang,<sup>1</sup> and Chang-De Gong<sup>1,2</sup>

<sup>1</sup>*Center for Statistical and Theoretical Condensed Matter Physics, and Department of Physics, Zhejiang Normal University, Jinhua 321004, China*

<sup>2</sup>*National Laboratory of Solid State Microstructures and Department of Physics, Nanjing University, Nanjing 210093, China*  
(Received 12 May 2012; revised manuscript received 18 July 2012; published 16 August 2012)

We study a tight-binding model on the two-dimensional star lattice (also called the decorated honeycomb lattice) with short-range hoppings modulated by staggered fluxes. We observe a series of topological quantum phase transitions when tuning the hopping parameters, and find nontrivial topological bands with high Chern numbers. We also find in some parameter regions, the system exhibits the interesting topological flat bands with large flatness ratios of the band gaps over the bandwidths. We further illustrate the 1/2 fractional quantum Hall effect of interacting hard-core bosons filled in a lowest topological flat band of the star lattice.

DOI: [10.1103/PhysRevB.86.085311](https://doi.org/10.1103/PhysRevB.86.085311)

PACS number(s): 73.43.Cd, 71.10.Ca, 73.43.Nq, 71.10.Fd

## I. INTRODUCTION

In the past several years, topological quantum states of matter have shed new light on the forefront of condensed matter physics. Haldane was pioneering to introduce a two-band tight-binding model on the two-dimensional (2D) honeycomb lattice with hopping integrals modulated by staggered magnetic fluxes,<sup>1</sup> and this simple two-band model is considered as the prototype example of topological band insulators.<sup>2,3</sup> There are two types of insulating states in the Haldane model when the lower band is fully filled and the upper band is empty, and the distinction between them is the topological property of the occupied lower band which is encoded into the Chern number.<sup>4</sup> A trivial Chern number  $C = 0$  corresponds to a normal band insulator, while a nontrivial Chern number  $C = \pm 1$  corresponds to a topological band insulator.

Topological bands with nonzero Chern numbers have also been found in some other two-dimensional lattice models which are the natural extensions of the original Haldane model, e.g., the checkerboard lattice,<sup>5-7</sup> the kagome lattice,<sup>8,9</sup> the Lieb lattice,<sup>10</sup> and the square-octagon lattice.<sup>11</sup> Recently, a series of lattice models with the nontrivial topological flat bands (TFBs)<sup>12-16</sup> have been proposed in some two-dimensional lattice systems. Proposals of TFBs have provided a possible route to realize the intriguing fractional quantum Hall effect (FQHE) without Landau levels (LLs) as demonstrated in the recent systematic numerical works.<sup>17-21</sup>

Here, we study a tight-binding model on the star lattice (also called the decorated honeycomb lattice or the triangle-honeycomb lattice) with staggered fluxes and short-range hoppings.<sup>22-24</sup> We discuss topological quantum phase transitions (TQPTs) when tuning the next-nearest-neighbor parameter  $t_2$  with the others being fixed, and observe some topological bands with high Chern numbers. Besides, we find that in some parameter regions, the system exhibits the interesting TFBs with a Chern number  $C = -1$  and a large gap above them, and the flatness ratio of the band gap over the bandwidth can be as high as 85. Such a TFB has also been demonstrated to be another ideal platform for realizing a robust 1/2 FQHE of interacting hard-core bosons without LLs<sup>18</sup> by the exact diagonalization (ED) method.

## II. MODEL AND FORMULATION

Consider a star lattice with three different hopping integrals and staggered magnetic fluxes. For the neighbor triangular lattices, the magnetic fluxes are the same with the value  $-3\phi_1$ , and the neighbor dodecagon lattices have the opposite sign with the value  $+6\phi_1$ , but the total magnetic fluxes of the whole star lattice are zero as shown in Fig. 1. This model is similar to the spinless (or spin-polarized) version of the star-lattice model with spin-orbit couplings.<sup>23,24</sup> The nearest-neighbor (NN) hopping  $t_1$  is complex; every triangular lattice has three NN bonds and between two triangular lattices, there is a NN bond. In addition, the next-nearest-neighbor (NNN) hopping  $t_2$  and the next-next-nearest-neighbor (NNNN) hopping  $t_3$  are also considered; every lattice point has four NNN bonds and NNNN bonds with the same magnitude in different directions as indicated. Note that there are two hexagonal lattices and three square lattices in every dodecagon lattice, we do not draw all bonds in Fig. 1. The tight-binding Hamiltonian of the star-lattice model is given by<sup>22-24</sup>

$$H_0 = t_1 \sum_{\langle i,j \rangle} (e^{i\phi_1} c_i^\dagger c_j + \text{H.c.}) + t_2 \sum_{\langle\langle i,j \rangle\rangle} (c_i^\dagger c_j + \text{H.c.}) + t_3 \sum_{\langle\langle\langle i,j \rangle\rangle\rangle} (c_i^\dagger c_j + \text{H.c.}), \quad (1)$$

where  $t_1$ ,  $t_2$ , and  $t_3$  are the NN, the NNN, and the NNNN hopping integral parameters, respectively, and the operator  $c_i^\dagger$  ( $c_i$ ) creates (annihilates) a spinless electron (or fermion) at the  $i$ th site. Here we set  $t_1 = 1$ , and  $\phi_1$  represents the phase of the NN bonds.

After the Fourier transformation and the numerical diagonalization of the Hamiltonian Eq. (1), the zero-temperature Hall conductance is given by the Kubo formula<sup>4</sup>

$$\sigma_H(E) = \frac{ie^2}{A\hbar} \sum_{\mathcal{E}_{n\mathbf{k}} < E} \sum_{\mathcal{E}_{m\mathbf{k}} > E} \frac{\langle n\mathbf{k}|v_x|m\mathbf{k}\rangle \langle m\mathbf{k}|v_y|n\mathbf{k}\rangle - \langle n\mathbf{k}|v_y|m\mathbf{k}\rangle \langle m\mathbf{k}|v_x|n\mathbf{k}\rangle}{(\mathcal{E}_{m\mathbf{k}} - \mathcal{E}_{n\mathbf{k}})^2}, \quad (2)$$

with the system area  $A = L \times L$ , the Fermi energy  $E$ , the eigenvalue  $\mathcal{E}_{n\mathbf{k}}$  and eigenstate  $|n\mathbf{k}\rangle$  of the  $n$ th energy band,

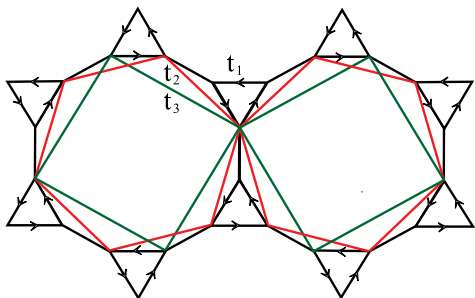


FIG. 1. (Color online) The star lattice with three different short-range hopping integrals, and each triangle and dodecagon is threaded by a staggered magnetic flux. Each NN bond has the phase  $\pm\phi_1$ , and the sign of the phase is represented by the arrow direction.

and the summation over  $\mathbf{k}$  is restricted to the first Brillouin zone (BZ). The velocity operator is defined as  $\mathbf{v} = (i/\hbar)[H, \mathbf{R}]$ , with  $\mathbf{R}$  as the position operator of electrons. When the Fermi energy  $E$  falls in energy gaps, we can rewrite  $\sigma_H$  as  $\sigma_H(E) = \sum_{\varepsilon_n < E} \sigma_H^{(n)} = e^2/h \sum_{\varepsilon_n < E} C_n$ , where  $\sigma_H^{(n)}$  and  $C_n$  are the Hall conductance and the Chern number<sup>4</sup> of the  $n$ th completely filled band, respectively.

### III. TOPOLOGICAL QUANTUM PHASE TRANSITIONS

We are interested in the possible TQPTs when tuning one parameter ( $t_2$ ) while the others are fixed ( $t_3, \phi_1$ ). Previously, TQPTs have also been studied in the star-lattice model with two kinds of NN hoppings<sup>22,23</sup> and with NNN spin-orbit couplings.<sup>23</sup> We here demonstrate a systematic evolution of the Hall conductances in the cases with the parameters  $t_3 = 0$  and  $\phi_1 = 0.5\pi$  while tuning  $t_2$  from 0.0 to 1.0. As shown in Fig. 2, it mainly experiences six evolution steps from Fig. 2(a) to Fig. 2(f). When  $t_2 = 0.0$ , the DOS have six clearly observable peaks, and among those peaks there are five plateaus with the Hall conductances  $\sigma_H = n(e^2/h)$ , ( $n = 1, 1, 1, 1, 1$ ) in Fig. 2(a). Correspondingly, there are six Chern numbers of each topological bands in sequence as  $C = \{+1, 0, 0, 0, 0, -1\}$ , which agree with the well-known result about a chiral spin liquid on the star lattice.<sup>22</sup> With  $t_2$  increased to 0.289, the first (lowest) two bands and the last (highest) two bands almost merge together and form pseudogaps [see Figs. 2(b) and 3(a)]; it is a critical point where a TQPT takes place with a quantized jump from the  $\sigma_H = +(e^2/h)$  integer quantum Hall effect (IQHE) plateau to the  $\sigma_H = -(e^2/h)$  IQHE plateau when the lowest band is totally filled while all the other higher-energy bands are empty (i.e.,  $1/6$  filling of the lattice). Then when  $t_2$  is increased to 0.40, the five well-defined IQHE plateaus with the Hall conductance  $\sigma_H = n(e^2/h)$  are also clearly shown in Fig. 2(c), where  $n = -1, 1, 1, 1, -1$ . The Chern numbers are redistributed as  $C = \{-1, +2, 0, 0, -2, +1\}$ . When  $t_2$  is further increased to 0.50, the second lowest band and the third lowest band begin to overlap with each other and share a total Chern number  $C = +2$ , while the lowest band has the Chern number  $C = -1$  [see Figs. 2(d) and 3(b)]. At  $t_2 = 0.545$ , the second lowest band and the third lowest band begin to split again and form a pseudogap at this critical point [see Fig. 2(e)]. It is very close to quantum critical points where TQPTs take place

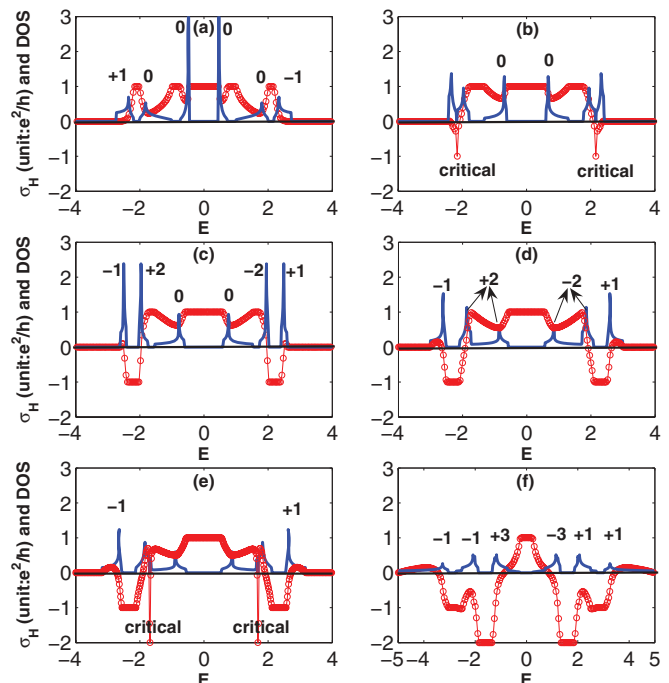


FIG. 2. (Color online) The Hall conductance  $\sigma_H$  (points) and the DOS (line) versus the Fermi energy with parameters  $t_3 = 0$  and  $\phi_1 = 0.5\pi$  for various  $t_2$ 's. And the Chern numbers of the six bands are also labeled. (a)  $t_2 = 0.0$ , (b)  $t_2 = 0.289$ , (c)  $t_2 = 0.40$ , (d)  $t_2 = 0.50$ , (e)  $t_2 = 0.545$ , (f)  $t_2 = 1.0$ .

from a gapped state with  $\sigma_H = +(e^2/h)$  IQHE plateau to a gapless state (with Fermi surfaces) and then to another gapped state with the  $\sigma_H = -(e^2/h)$  IQHE plateau when the lowest two bands are totally filled (i.e.,  $1/3$  filling of the lattice). When  $t_2$  is further increased to 1.0, the middle energy gap becomes more and more narrow, and the sequential Chern numbers are redistributed as  $C = \{-1, -1, +3, -3, +1, +1\}$ . The evolutions of Chern numbers of corresponding topological bands have revealed various topological insulating phases. Interestingly, topological phases with high Chern numbers

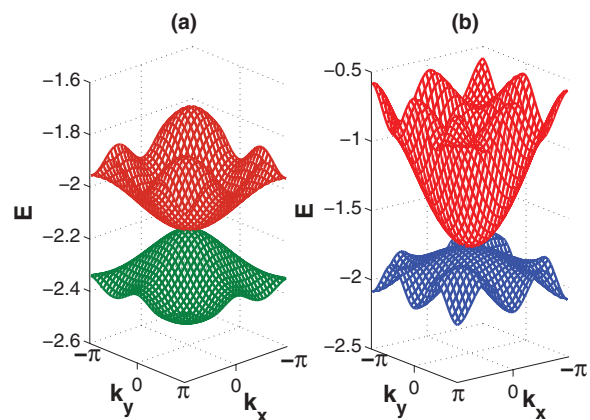


FIG. 3. (Color online) (a) Two lower bands structure for the star lattice with the parameters  $t_2 = 0.289$ ,  $t_3 = 0$ ,  $\phi_1 = 0.5\pi$ . (b) The second band and the third band structure for the star lattice with the parameters  $t_2 = 0.50$ ,  $t_3 = 0$ ,  $\phi_1 = 0.5\pi$ .

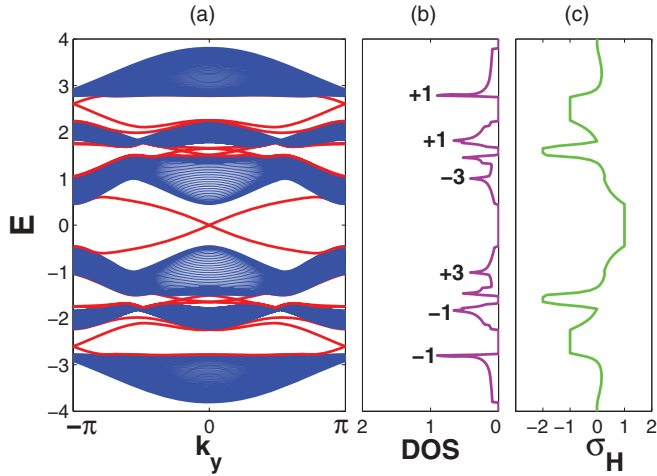


FIG. 4. (Color online) (a) Topological band structures and edge states for the star lattice on a cylinder with the parameters  $t_2 = 0.70$ ,  $t_3 = 0, \phi_1 = 0.5\pi$ . (b) The DOS and Chern numbers for the spectrum in (a). (c) The Hall conductance in units of  $e^2/h$ .

may also appear at half fillings of the star lattice with NNN spin-orbit couplings.<sup>23</sup>

It is interesting to note that there are quadratic band crossings at the  $(k_x, k_y) = (0, 0)$   $\Gamma$  point<sup>7</sup> between the corresponding two bands at  $t_2 = 0.289$  [Fig. 3(a)] and at  $t_2 = 0.50$  [Fig. 3(b)]. It is also noteworthy that when tuning parameter  $t_2$  from 0.50 to 0.545, it forms a circular Fermi pocket centered at the  $\Gamma$  point (as similar as the Fermi pocket centered at the  $K$  point in the BZ boundary of a kagome-lattice model<sup>25</sup>) between the second lowest band and the third lowest band (these two bands overlap with each other).

An alternative way to reveal topological properties and TQPTs is to calculate the edge states. The Chern numbers of the bulk bands are intimately related to the winding numbers of the corresponding edge states.<sup>26</sup> There is also a correspondence between the quantized jumps of  $\sigma_H$  and the topological evolutions of bulk spectra. Now we show a typical example of topological bands with high Chern numbers (see Fig. 4). We take a cylinder of the star lattice model with a 64-unit-cell open boundary condition in the  $x$  direction and a periodic boundary condition in the  $y$  direction, and depict edge states among the six bulk bands. We can see that when the Fermi energy is zero (1/2 filling of the lattice), namely the third band is fully occupied while the other higher bands are empty, it drives the model into a topological insulating phase with a  $C = +3$  valence band.

#### IV. TOPOLOGICAL FLAT BANDS

It is extensively reported that FQH states will occur in 2D lattice systems when the TFBs<sup>12-16</sup> are fractionally filled with interacting particles.<sup>17-21</sup> A TFB with a large flatness ratio (the ratio of band gap over bandwidth) is a crucial condition for the occurrence of the FQHE. We are now interested in obtaining TFBs with nonzero Chern numbers and large flatness ratios in the star lattice model.

Focusing on the nontrivial lowest band with the Chern number  $C = -1$ , we look for the regimes in which this lowest

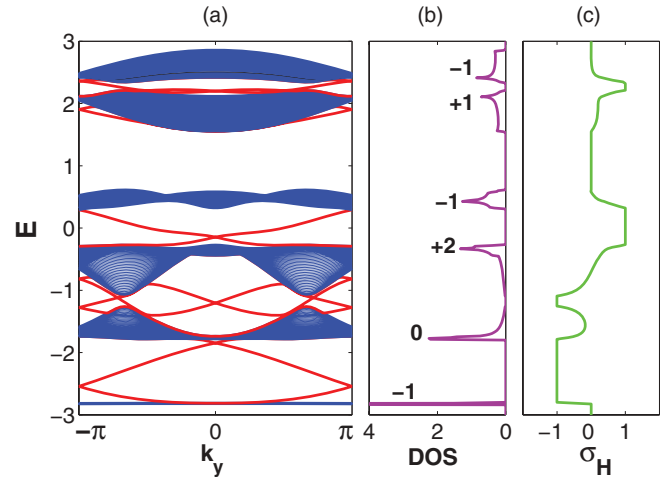


FIG. 5. (Color online) (a) TFB structures and edge states for the star lattice on a cylinder with the parameters  $t_2 = 0.3$ ,  $t_3 = -0.25$ ,  $\phi_1 = 0.6\pi$ . The spectrum have a band gap  $\Delta \approx 1.031$ , the bandwidth of the lowest band  $W \approx 0.012$ , flatness  $\Delta/W \approx 85$ . (b) The DOS and Chern numbers for the spectrum in (a). (c) The Hall conductance in units of  $e^2/h$ .

band is very flat compared to the band gap. Here, we show a typical example of lowest TFBs in the presence of the NNNN hopping integral  $t_3$ . In Fig. 5, the band gap between the lowest two bands is  $\Delta \approx 1.031$ ; the bandwidth of the lowest TFB is very narrow and has the value  $W \approx 0.012$ . In Fig. 6, the band gap between the lowest two bands is  $\Delta \approx 0.2$ ; the bandwidth of the lowest TFB is also very narrow and has the value  $W \approx 0.005$ . We denote  $\Delta = E_{2,\min}(\mathbf{k}) - E_{1,\max}(\mathbf{k})$  [see Fig. 7(b)],  $W = E_{1,\max}(\mathbf{k}) - E_{1,\min}(\mathbf{k})$ , where  $E_2(\mathbf{k})$  and  $E_1(\mathbf{k})$  represent the energy spectra of the second lowest band and the lowest band, respectively. Our results about these TFBs are based upon the explicit calculations of the energy spectrum, the

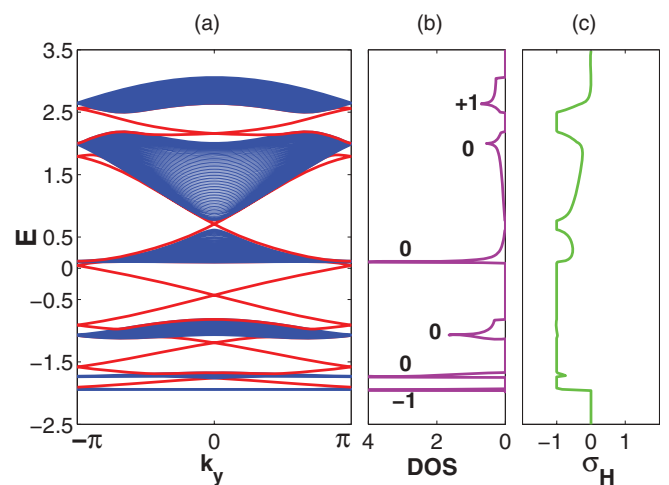


FIG. 6. (Color online) (a) TFB structures and edge states for the star lattice on a cylinder with the parameters  $t_2 = -0.14$ ,  $t_3 = 0.06$ ,  $\phi_1 = 0.77\pi$ . The spectrum have a band gap  $\Delta \approx 0.2$ , the bandwidth of the lowest band  $W \approx 0.005$ , flatness  $\Delta/W \approx 40$ . (b) The DOS and Chern numbers for the spectrum in (a). (c) The Hall conductance in units of  $e^2/h$ .

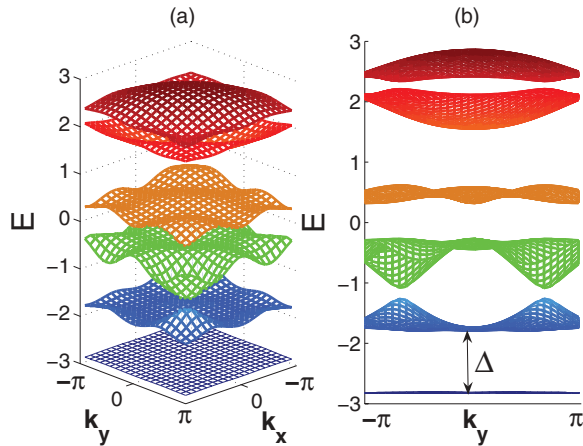


FIG. 7. (Color online) (a) The spectrum for the star lattice with the parameters  $t_2 = 0.3$ ,  $t_3 = -0.25$ ,  $\phi_1 = 0.6\pi$ . (b) Section graph of the spectrum (a); band gap  $\Delta$  is depicted in the graph.

density of state, the Hall conductance, as well as the edge-state spectrum.

Previously, some many-body phases such as chiral spin liquids of interacting spins<sup>22</sup> and topological insulating states and symmetry-breaking phases of interacting fermions have been studied in the star-lattice model.<sup>23,24</sup> Here as an illustration of possible many-body fractional topological phases<sup>17-21</sup> in the star lattice, we consider filling interacting hard-core bosons into a lowest TFB and expect possible bosonic FQHE at fractional fillings.<sup>18</sup> In our ED study, we consider a finite system of  $N_x \times N_y$  unit cells (total number of sites  $N_s = 6 \times N_x \times N_y$ ) with periodic boundary conditions, denoting the number of hard-core bosons as  $N_b$ , and the filling factor of a TFB is thus  $N_b/(N_x N_y)$ . We diagonalize the many-body Hamiltonian in each momentum  $\mathbf{q} = (2\pi k_x/N_x, 2\pi k_y/N_y)$  sector, with  $(k_x, k_y)$  as integer quantum numbers. A few lowest states in each momentum sector of three system sizes with  $N_s = 36$  ( $6 \times 2 \times 3$ ), 48 ( $6 \times 2 \times 4$ ), and 60 ( $6 \times 2 \times 5$ ), at the  $1/2$  filling of the lowest TFB with the flatness ratio 85 (Fig. 7), are shown in Fig. 8. We can see that, for each system size, there is an obvious ground state manifold (GSM) with two-fold quasidegenerate ground states, and the GSM is well separated from the higher energy spectrum by a large gap, which characterizes a robust  $1/2$  FQHE.<sup>18</sup>

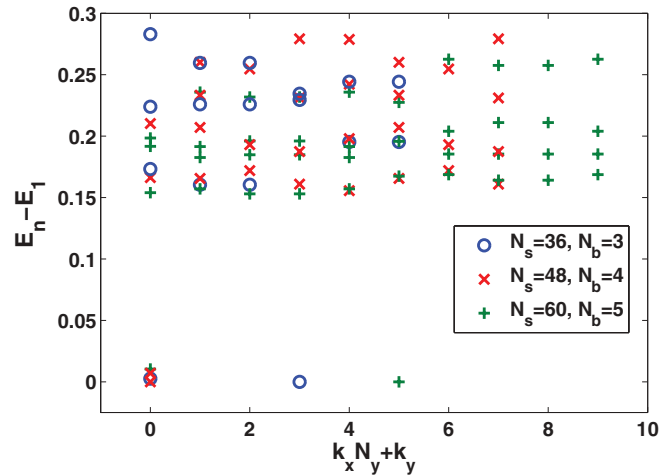


FIG. 8. (Color online) The  $1/2$  bosonic FQHE. Low energy spectrum  $E_n - E_1$  versus the momentum  $k_x N_y + k_y$  for three lattice sizes  $N_s = 36, 48, 60$  and hard-core boson numbers  $N_b = 3, 4, 5$  with the parameters  $t_2 = 0.3$ ,  $t_3 = -0.25$ ,  $\phi_1 = 0.6\pi$ .

## V. SUMMARY AND DISCUSSION

In summary, we have demonstrated the interesting process of TQPTs by tuning parameter  $t_2$  while the other parameters  $t_3$  and  $\phi_1$  are fixed, have shown some topological bands with high Chern numbers, and have found that some interesting TFBs with large flatness ratios occur in some proper parameters by numerical calculations. We also illustrate that  $1/2$  FQHE of interacting hard-core bosons filled in a lowest TFB of the star lattice, with signatures of two-fold quasidegenerate ground states on a torus and a robust spectrum gap separating them from the higher energy spectrum by the ED method. Such TQPTs and TFBs in this star-lattice model might be possible to be realized in optical lattices by manipulating cold atoms,<sup>27-29</sup> considering the very recent experimental advances of creating artificial staggered gauge fields.<sup>30,31</sup>

## ACKNOWLEDGMENTS

This work is supported by the NSFC of China Grant No. 10904130 (Y.F.W.), and the State Key Program for Basic Researches of China Grants No. 2006CB921802 and No. 2009CB929504 (C.D.G.).

<sup>1</sup>F. D. M. Haldane, *Phys. Rev. Lett.* **61**, 2015 (1988).

<sup>2</sup>M. Z. Hasan and C. L. Kane, *Rev. Mod. Phys.* **82**, 3045 (2010).

<sup>3</sup>X.-L. Qi and S.-C. Zhang, *Rev. Mod. Phys.* **83**, 1057 (2011).

<sup>4</sup>D. J. Thouless, M. Kohmoto, M. P. Nightingale, and M. den Nijs, *Phys. Rev. Lett.* **49**, 405 (1982).

<sup>5</sup>V. M. Yakovenko, *Phys. Rev. Lett.* **65**, 251 (1990).

<sup>6</sup>F. X. Li, L. Sheng, and D. Y. Xing, *Europhys. Lett.* **84**, 60004 (2008).

<sup>7</sup>K. Sun, H. Yao, E. Fradkin, and S. A. Kivelson, *Phys. Rev. Lett.* **103**, 046811 (2009).

<sup>8</sup>K. Ohgushi, S. Murakami, and N. Nagaosa, *Phys. Rev. B* **62**, R6065 (2000).

<sup>9</sup>H. M. Guo and M. Franz, *Phys. Rev. B* **80**, 113102 (2009).

<sup>10</sup>C. Weeks and M. Franz, *Phys. Rev. B* **82**, 085310 (2010).

<sup>11</sup>M. Kargarian and G. A. Fiete, *Phys. Rev. B* **82**, 085106 (2010).

<sup>12</sup>E. Tang, J. W. Mei, and X. G. Wen, *Phys. Rev. Lett.* **106**, 236802 (2011).

<sup>13</sup>K. Sun, Z. Gu, H. Katsura, and S. Das Sarma, *Phys. Rev. Lett.* **106**, 236803 (2011).

<sup>14</sup>T. Neupert, L. Santos, C. Chamon, and C. Mudry, *Phys. Rev. Lett.* **106**, 236804 (2011).

- <sup>15</sup>X. Hu, M. Kargarian, and G. A. Fiete, *Phys. Rev. B* **84**, 155116 (2011).
- <sup>16</sup>C. Weeks and M. Franz, *Phys. Rev. B* **85**, 041104 (2012).
- <sup>17</sup>D. N. Sheng, Z. C. Gu, K. Sun, and L. Sheng, *Nature Commun.* **2**, 389 (2011).
- <sup>18</sup>Y. F. Wang, Z. C. Gu, C. D. Gong, and D. N. Sheng, *Phys. Rev. Lett.* **107**, 146803 (2011).
- <sup>19</sup>N. Regnault and B. A. Bernevig, *Phys. Rev. X* **1**, 021014 (2011).
- <sup>20</sup>Y. F. Wang, H. Yao, Z. C. Gu, C. D. Gong, and D. N. Sheng, *Phys. Rev. Lett.* **108**, 126805 (2012).
- <sup>21</sup>Y. L. Wu, B. A. Bernevig, and N. Regnault, *Phys. Rev. B* **85**, 075116 (2012).
- <sup>22</sup>H. Yao and S. A. Kivelson, *Phys. Rev. Lett.* **99**, 247203 (2007).
- <sup>23</sup>A. Rüegg, J. Wen, and G. A. Fiete, *Phys. Rev. B* **81**, 205115 (2010).
- <sup>24</sup>J. Wen, A. Rüegg, C. C. Joseph Wang, and G. A. Fiete, *Phys. Rev. B* **82**, 075125 (2010).
- <sup>25</sup>V. Chua, H. Yao, and G. A. Fiete, *Phys. Rev. B* **83**, 180412 (2011).
- <sup>26</sup>Y. Hatsugai, *Phys. Rev. Lett.* **71**, 3697 (1993).
- <sup>27</sup>C. Wu, *Phys. Rev. Lett.* **101**, 186807 (2008).
- <sup>28</sup>L. B. Shao, S. L. Zhu, L. Sheng, D. Y. Xing, and Z. D. Wang, *Phys. Rev. Lett.* **101**, 246810 (2008).
- <sup>29</sup>T. D. Stanescu, V. Galitski, J. Y. Vaishnav, C. W. Clark, and S. Das Sarma, *Phys. Rev. A* **79**, 053639 (2009); T. D. Stanescu, V. Galitski, and S. Das Sarma, *ibid.* **82**, 013608 (2010).
- <sup>30</sup>M. Aidelsburger, M. Atala, S. Nascimbene, S. Trotzky, Y. A. Chen, and I. Bloch, *Phys. Rev. Lett.* **107**, 255301 (2011).
- <sup>31</sup>J. Struck, C. Olschlager, M. Weinberg, P. Hauke, J. Simonet, A. Eckardt, M. Lewenstein, K. Sengstock, and P. Windpassinger, *Phys. Rev. Lett.* **108**, 225304 (2012).